Available online at www.sciencedirect.com
SCIENCE DIRECT®

Journal of the European Ceramic Society 24 (2004) 821–824

www.elsevier.com/locate/jeurceramsoc

^{57}Fe Mössbauer and electronic spectroscopy study on a new synthetic hercynite-based pigment

Giovanni B. Andreozzi[a], Giovanni Baldi[b], Gian Piero Bernardini[c], Francesco Di Benedetto[c,*], Maurizio Romanelli[d]

[a]*Dipartimento di Scienze della Terra, Università di Roma "La Sapienza", Roma, 00185 Italy*
[b]*Laboratorio di Ricerca Avanzata, Gruppo Colorobbia, Sovigliana, Firenze, 50053 Italy*
[c]*Dipartimento di Scienze della Terra, Università di Firenze, Firenze, 50121 Italy*
[d]*Dipartimento di Chimica, Università di Firenze, Firenze, 50019 Italy*

Received 25 January 2003; accepted 21 April 2003

Abstract

A new blue hercynite-based pigment, stable at the processing temperatures for the ceramic application, has been synthesized. It is constituted by corundum and Ti-bearing hercynite. In order to clarify the complex Fe distribution evidenced by Baldi et al. [Proc. CIMTEC 2002(2003)], a ^{57}Fe Mössbauer and diffuse reflectance spectroscopy study has been undertaken. Fe was found to be distributed between corundum, as trivalent, and hercynite, both as Fe(II) and Fe(III). Moreover, Fe(II) occupies both tetrahedral and octahedral sites in the latter mineral, according to a temperature dependent disorder. UV–VIS investigation revealed the presence of a broad band in the blue region, the shape and position of which was found to be due to an intervalence charge transfer mechanism between Fe(II) and Ti(IV) in two edge-sharing octahedra of hercynite.

Keywords: Al_2O_3; Colour; Pigment; Spectroscopy; Spinels

1. Introduction

Ceramic pigments are white or coloured crystalline materials with high thermal stability and high chemical resistance. These properties are strategic for their use in high temperature treatments. In recent years the development of new ceramic materials has fostered the research of pigments stable at application temperatures over 1200 °C. The crystalline coloured substances that remain unaltered in such conditions belong to a restricted number of structures: zirconium silicate $ZrSiO_4$, spinels $M^{II}M^{III}_2O_4$, corundum Al_2O_3 and rutile TiO_2 can be mentioned, thus leading to further limitations in the colours which can be achieved: for example cobalt-zinc aluminate spinels $CoAl_2O_4$ and $(Co,Zn)Al_2O_4$ are the only high-temperature blue pigments widely used in ceramic industry.

A research project pointing to increase the number of blue high temperature ceramic pigments and lower production costs is going on in the Laboratorio di Ricerca Avanzata, Gruppo Colorobbia. A new, deep blue pigment based on hercynite spinel structure is synthesized. It contains Fe and Ti and shows good chromatic stability at high temperature in reducing conditions.

To fully understand colouring properties of such a pigment, the oxidation state and actual intracrystalline distribution of Fe and Ti must be determined. It has already been proved, in fact, that temperature-dependent partitioning of Fe^{2+} and Fe^{3+} between the tetrahedral, T, and octahedral, M, sites strongly affects optical absorption spectra of spinel solid solutions.[2,3] In order to accurately determine intracrystalline Fe distribution of this new pigment and to clarify the nature of its blue colour, ^{57}Fe Mössbauer and electronic diffuse reflectance spectra were recorded.

2. Materials and experimental procedures

The pigment was prepared by carefully mixing commercial reagents: α-alumina, <45 μ Merck ppa, $(NH_4)_2TiO(SO_4)_2$, Merck ppa, and $(NH_4)_2Fe(SO_4)_2$,

* Corresponding author.
E-mail address: dibenefr@geo.unifi.it (F. Di Benedetto).

0955-2219/03/$ - see front matter © 2003 Elsevier Ltd. All rights reserved.
doi:10.1016/S0955-2219(03)00329-7

Merck ppa. The mixture was heated in a high temperature furnace (Linn-1700 °C) in zirconia crucible with a total thermal treatment of 8 h and a plateau of 2 h at 1450 °C. The reaction chamber was saturated with a mixture of $Ar–H_2$ 96%–4% and the reducing atmosphere maintained all over the time of thermal treatment: a deep-blue coloured powder was obtained after cooling.

The sample was further powdered in an alumina crucible down to 30 μm, and checked by means of X-ray diffraction, using a Philips PW1710 diffractometer with Cu anode equipped with PC-APD software for data acquisition and handling. Experimental conditions were: 10–140° 2θ, step size 0.05° 2θ, 2 s per step.

Microchemical analyses were performed through a Jeol JXA8600 electron microprobe (EMP), operating at 10 nA and 15 kV, with counting times 15 s on peaks and 10 s on backgrounds. Crystals used as standards were: ilmenite ($FeTiO_3$) for Ti and Fe and a commercial plagioclase (Astimex Ltd.) for Al. The absorber for Mössbauer spectroscopy was prepared by pressing a finely ground sample with a powdered acrylic resin (lucite) to self-supporting discs. A 50 mg sample was used, so as to have an absorber with Fe thickness in the range 1–2 mg/cm^2. Spectra were collected both at room and at liquid nitrogen temperature using a conventional spectrometer system operating in constant acceleration mode with a ^{57}Co source of nominal 50 mCi in rhodium matrix. Spectral data for the velocity range −4 to 4 mm/s were recorded in a multichannel analyser using 512 channels. After velocity calibration against a spectrum of high-purity α-iron foil (25 μm thick), the raw data were folded to 256 channels. The spectra were fitted assuming Lorentzian peak shape and using the fitting program Recoil 1.04. Reduced χ^2 was used as parameter to evaluate statistical best fit, and uncertainties were calculated using the covariance matrix. Errors are estimated at about ±0.02 mm/s for isomer shift (IS), quadrupole splitting (QS), and peak full width at full maximum and no less then ±3% for doublet areas.

Diffuse reflectance spectroscopy (DRS) investigations were performed in the UV and VIS range by means of a Lambda 900 UV/VIS/NIR spectrometer, with double radiation (deuterium and tungsten for UV and visible regions, respectively), monochromators in Littrow geometry and the use of an integration sphere. Spectra, collected on powders pressed on a black tape, which was used also as reference, were acquired from 800 to 190 nm with a step size of 1 nm. Spectral absorptions were fitted assuming gaussian line shapes by means of a least squares algorithm (included in Microcal Origin 6.0 package).

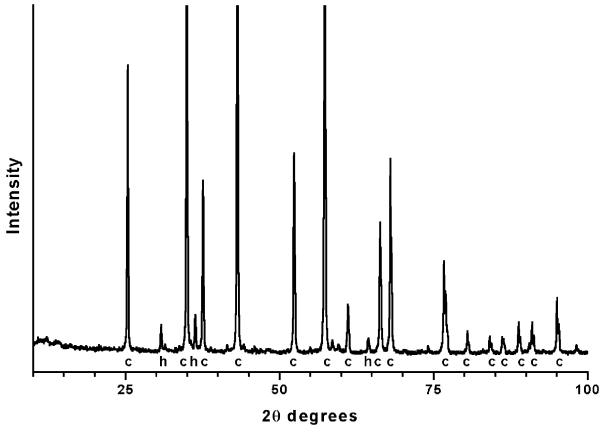

Fig. 1. XRD powder pattern of the blue pigment: hercynite (h), corundum (c).

3. Results and discussion

3.1. Mineralogical and chemical composition

From inspection of powder XRD pattern, reported in Fig. 1, the pigment was found to be polyphasic containing corundum, Al_2O_3, and hercynite, $FeAl_2O_4$, this latter being a minor constituent (<10 wt.%). Quantitative analysis of the patterns by means of Rietveld algorithm was not carried out due to *iso*-orientation of minor constituents, which would have caused high uncertainty in wt.% determination.

Refined lattice parameter a of hercynite equals 8.162 Å, not in good agreement with that reported in the JCPDS 34-192 file (8.153 Å). However, such a parameter may account for the minor Ti content and also for a possible small amount of ferric iron, as already observed in synthetic hercynite.[4]

Microanalyses performed by EMP (Table 1) could not determine the actual ferric iron content of hercynite grains in the blue pigment, but confirmed contents of Ti up to 0.06 atoms per formula unit (apfu) substituting for both Al and Fe. The chemical formula of hercynite calculated from microchemical analyses is, therefore, $Fe_{0.97}Ti_{0.06}Al_{1.94}O_4$.

3.2. Spectroscopic characterization

Liquid nitrogen Mössbauer spectrum of blue pigment is dominated by a broad absorption band with IS close to 1 mm/s and variable QS values between 1 and 3 mm/s

Table 1
Mean values of XRPD and EMP data for hercynite in the blue pigment

XRPD a(Å)	EMP			
	FeO (wt.%)	TiO_2 (wt.%)	Al_2O_3 (wt.%)	Sum (wt.%)
8.162 (2)	40.80 (46)	2.80 (8)	58.33 (6)	101.93 (59)

(Fig. 2). In agreement with the existing literature (see e.g. Ref.3), this part of the absorption envelope is considered to be due to ferrous iron. In the spinel structure Fe(II) mainly populates the tetrahedrally-coordinated T site, which is surrounded by 12 octahedral sites. Due to heterogeneous cation population in octahedral sites, a broad absorption of Fe(II) doublets can be expected.[5] A weak band due to ferric iron is also present in the spectrum. This band, not resolved, contributes to the low-velocity half of the spectrum, which has a larger absorption area than the high-velocity half.

Several fitting strategies were tested to find a model that could be used with as few constraints as possible. The final model consisted of three outer doublets representing the broad tetrahedrally-coordinated Fe^{2+} contribution (77% of Fe_{tot}), one inner doublet for the octahedrally-coordinated Fe(II) contribution (10% of Fe_{tot}), and two weak doublets due to Fe(III). The obtained hyperfine parameters are listed in Table 2. The fitting model is the same as used by Halenius et al.[3] for synthetic spinel–hercynite samples and is very similar to the one used by Waerenborgh et al.[6] for gahnite–hercynite samples, although the latter authors used a quadrupole splitting distribution for the $^{IV}Fe^{2+}$ absorption feature.

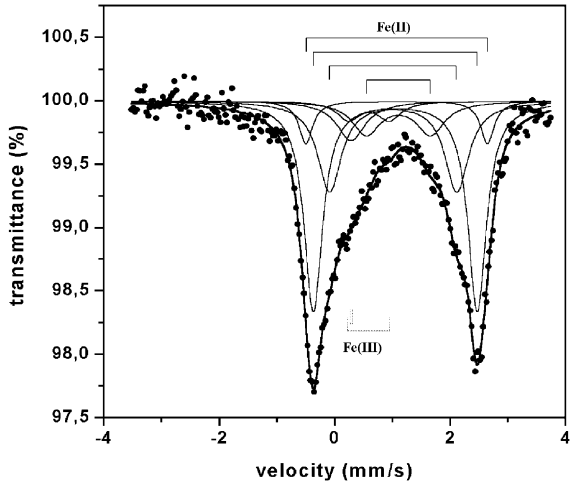

Fig. 2. Liquid nitrogen ^{57}Fe Mössbauer spectrum of the blue pigment. Continuous lines are the fitted components.

With reference to Fe(III) doublets, the one with IS 0.46 mm/s and QS 1.25 mm/s was tentatively attributed to ferric iron in the regular octahedron of hercynite structure, but the relative area is so small (<1% of Fe_{tot}) that its actual presence is questionable. The second one, with IS 0.51 mm/s and QS 0.31 mm/s, is typical of a more distorted coordination with a relatively homogeneous next-nearest neighbourhood. Considering that this Fe(III) doublet is about 12% of Fe_{tot} and corundum is more than 90% of bulk pigment, such a doublet may be attributed to very diluted Fe(III) in the corundum structure.

Optical absorption spectrum of deep blue pigment was compared with a "blank", the analogous Ti-free mixture already analysed by Baldi et al.[1] DRS spectra of both samples are shown in Fig. 3, where the deep blue pigment is labeled as S_A and the white Ti-free pigment as S_B. No large differences may be identified in the UV region, where the two main bands, centered, respectively, at 207.0(1) and 264.1(1) nm in sample S_A and 201.8(1) and 258.9(2) nm in sample S_B, should be attributed to Fe–O charge transfer processes.[7] On the contrary, very large differences may be observed in the VIS region (400–800 nm): a wide band at 579(6) nm with a shoulder at 737(10) nm dominates S_A spectrum but is absent in S_B spectrum.

Burns,[8] studying natural and synthetic blue sapphires, evidenced the presence of an absorption with a very similar structure responsible for the blue colour. In sapphire the absorption was attributed to inter-valence charge transfer (IVCT) transitions between Fe(II) and Ti(IV) across edge-sharing octahedra, with cation–cation

Table 2
Room temperature and liquid nitrogen ^{57}Fe Mössbauer data of the blue pigment sample

	IS	QS	FWHM	Area	Attribution
Room temperature					
1	0.90	2.18	0.24	37	Fe(II)
2	0.88	1.61	0.23	31	Fe(II)
3	0.91	0.95	0.21	21	Fe(II)
4	0.47	0.36	0.19	11	Fe(III)
Liquid nitrogen					
1	1.07	3.17	0.14	7	Fe(II)
2	1.05	2.85	0.18	39	Fe(II)
3	1.03	2.23	0.29	31	Fe(II)
4	0.99	1.40	0.29	10	Fe(II)
5	0.46	1.25	0.11	1	Fe(III)
6	0.51	0.31	0.30	12	Fe(III)

All hyperfine parameters are in mm/s except area (%); errors are estimated ±0.02 mm/s for IS (isomer shift), QS (quadrupole splitting), HWHM (full width at full maximum) and ±3% for area.

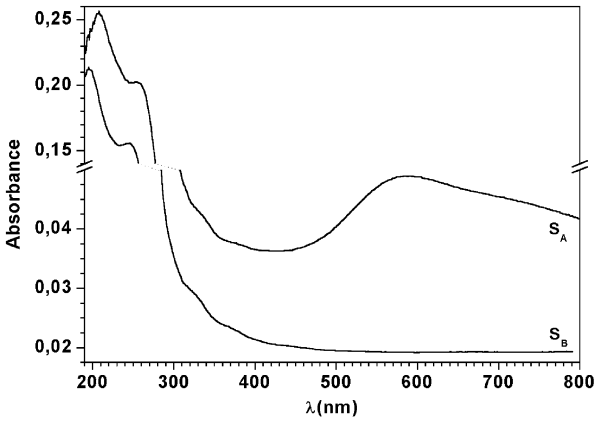

Fig. 3. Room temperature UV–vis DRS spectra of the blue pigment (S_A) and the white Ti-free analogous (S_B).

distance of ~2.88 Å. In case of IVCT transitions between the same ions in face-sharing octahedra (instead of edge-sharing), the interatomic distance decreases and the absorption would be shifted towards highest wavelength values (> 700 nm). Another possibility could be the attribution of the band observed at 579 nm to Fe(II)–Fe(III) IVCT transition, but Burns[8] definitively ruled out this possibility, and successively Hålenius et al.[3] found this last transition to cause absorption at 689 and 1052 nm in Fe^{3+}-bearing spinel–hercynite crystals.

4. Conclusions

In the deep blue pigment analysed, Fe(III)-bearing corundum and Ti-bearing hercynite are the only phases which could contribute to the interaction with VIS radiation. Since Fe-bearing corundum is present both in the deep blue pigment and in the Ti-free white pigment,[1] its contribution cannot explain the large difference in the diffuse reflectance spectra of the two materials. Moreover, due to the dilution of Fe(III) in corundum (less than 0.01 apfu), the spin-forbidden 3d transition should not substantially affect the VIS spectra. Its characteristic absorption, in fact, which should be visible in the range 380–450 nm,[8] has not been revealed in DRS spectra. Therefore, Ti-bearing hercynite is the only candidate for the blue colour.

In order to verify the analogy between optical spectra of blue pigment and sapphire, the IVCT transitions between Fe(II) and Ti(IV) across edge-sharing octahedra must occur in hercynite. Electron paramagnetic resonance (EPR) spectra collected on the same materials[1] ruled out the presence of Ti(III); the Ti measured by EMP in hercynite grains, therefore, is Ti(IV). In spinels, due to octahedral site preference of Ti and temperature-dependent Fe(II)-Al disorder, two edge-sharing octahedra may be occupied by Fe(II) and Ti(IV) at a distance very favourable for IVCT transition.[4,9,10] Since in hercynite the geometry of the Fe–Ti pair is the same as observed by Burns[8] in sapphire, it may be concluded that a Fe(II)–Ti(IV) IVCT transition originates the blue colour of the pigment.

Due to the low yield of hercynite in the pigment, further researches to increase hercynite content, in conditions characteristic for an industrial ceramic process, are in progress.

Acknowledgements

The authors wish to acknowledge F. Olmi, IGG-CNR, for the microanalytical data and G. Graziani, Università "La Sapienza", Roma, for the management of Mössbauer laboratory. A. Bencini and A. Dei, Università di Firenze, are also gratefully acknowledged for the fruitful discussion.

References

1. Baldi, G., Barzanti, A., Bernardini, G. P., Di, Benedetto, F., Faso, V. and Romanelli, M., Spectroscopic characterization of a new synthetic hercynite-based pigment. *Adv. Sci. Tech.*, 2003, **34**, 299–302.
2. Andreozzi, G. B., Hålenius, U. and Skogby, H., Spectroscopic active $^{IV}Fe^{3+}$–$^{VI}Fe^{3+}$ clusters in spinel magnesioferrite solid solution crystals: a potential monitor for ordering in oxide spinels. *Phys. Chem. Minerals*, 2001, **28**, 435–444.
3. Hålenius, U., Skogby, H. and Andreozzi, G. B., Influence of cation distribution on the optical absorption spectra of Fe^{3+} -bearing spinel s s.—hercynite crystals: evidence for electron transitions in $^{VI}Fe^{2+}$–$^{VI}Fe^{3+}$ clusters. *Phys. Chem. Minerals*, 2002, **29**, 319–330.
4. Andreozzi, G. B. and Lucchesi, S., Intersite distribution of Fe^{2+} and Mg in the spinel (sensu stricto)-hercynite series by single-crystal X-ray diffraction. *Amer. Min.*, 2002, **87**, 1113–1120.
5. Waerenborgh, J. C., Annersten, H., Ericsson, T., Figueiredo, M. O. and Cabral, J. M. P., A Mössbauer study of natural gahnite spinels showing strongly temperature-dependent quadrupole splitting distributions. *Eur. J. Mineral*, 1990, **2**, 267–271.
6. Waerenborgh, J. C., Figueiredo, M. O., Cabral, J. M. P. and Pereira, L. C. J., Powder XRD structure refinements and ^{57}Fe Mossbauer effect study of synthetic $Zn_{1-x}Fe_xAl_2O_4$ ($0 < x \leqslant 1$) spinels annealed at different temperatures. *Phys. Chem. Minerals*, 1994, **21**, 460–468.
7. Djemai, A., Calas, G. and Muller, J. P., Role of structural Fe(III) and iron oxide nanophases in mullite coloration. *J. Am. Ceram. Soc.*, 2001, **84**(7), 1627–1631.
8. Burns, R., Mineralogical applications of crystal field theory; 2nd edn. A. Putnis, R. C., Liebermann, 1993, Cambridge University Press.
9. Lucchesi, S. and Della Giusta, A., Crystal chemistry of non-stoichiometric Mg–Al synthetic spinels. *Z. Kristall*, 1994, **209**, 714–719.
10. Lavina, B., Salviulo, G. and Della Giusta, A., Cation distribution and structure modelling of spinel solid solutions. *Phys. Chem. Minerals*, 2002, **29**, 10–18.